Tellus (2000), 52A, 380–390
Printed in UK. All rights reserved

TELLUS
ISSN 0280–6495

Linear dynamics of hydrostatic adjustment to horizontally homogeneous heating

By AARNOUT VAN DELDEN*, *Institute for Marine and Atmospheric Research, Utrecht University, Princetonplein 5, 3584 CC Utrecht, The Netherlands*

(Manuscript received 23 February 1999; in final form 26 January 2000)

ABSTRACT

The process of hydrostatic adjustment to horizontally homogeneous heating in a stably stratified atmosphere of arbitrary thermal structure is investigated in the limit of small perturbations. A linear differential equation is derived for the vertical pressure distribution in the final balanced state. Solutions of this equation are compared with the time dependent solution which is found by numerically integrating the equations in time. During the process of hydrostatic adjustment acoustic-buoyancy oscillations are generated. The amplitudes of these oscillations become so great that static instability is generated at heights above 100 km, depending on where and how abruptly the heat is added. As a crude representation of the unstable breakdown and damping of these waves, Rayleigh damping is introduced. If the associated damping coefficient in the upper atmosphere is sufficiently large (greater than the Brunt Väisälä frequency), the oscillations vanish. Below a height of about 50 km the steady state predicted by the above mentioned differential equation is reached approximately in 10 min.

1. Introduction

If part of the atmosphere is heated, pressure and potential temperature in the heated air increase. The normal state of (hydrostatic) balance between the vertical pressure gradient force and the buoyancy force is disturbed. The heated air subsequently expands and pushes the air in the environment upwards and sideways. A process of readjustment to hydrostatic balance follows. Important questions concerning this process are the following. Is a steady state of hydrostatic balance reached? If so, what are the vertical pressure and potential temperature distributions in the final balanced state? How far above the heat-source is the pressure affected after the process of readjustment has been completed? How much time does the adjustment require?

In a series of papers Bannon (1995, 1996) investigated the prototype problem of hydrostatic adjustment for large scale atmospheric motions. This problem consists of the response of a stably stratified atmosphere to a vertically confined but horizontally uniform instantaneous heating. This problem was originally advanced by Lamb (1908) (see also Lamb, 1932, sections 309–311) and has therefore been termed "Lamb's problem" by Bannon. In fact, Lamb only investigated the properties of the waves excited by a point source of hydrostatic imbalance. These waves were termed "waves of expansion" by Lamb (1932). Bannon (1995) investigated the subsequent adjustment of the fluid for an isothermal atmosphere. In particular, inspired by Gill's (1982) linear technique of tackling the geostrophic adjustment problem, he derived an equation for the pressure as a function of height in the final equilibrium state. For an isothermal atmosphere he found that the pressure below the heat source is unaffected by the heating, whereas the pressure above the heat source is

* e-mail: a.j.vandelden@phys.uu.nl

increased compared to the initial value immediately after the heating. The pressure-increase is greatest at the top of the heated layer and decreases exponentially above the heated layer. The *e*-folding distance associated with this exponential decrease is proportional to the density scale height in an isothermal atmosphere, $H_S \equiv RT/g$, where R is the ideal gas constant, T the temperature and g the acceleration due to gravity. This characteristic depth scale can, by analogy to the radius of deformation for geostrophic adjustment, be referred to as the *radius of deformation for hydrostatic adjustment,* or perhaps better as the *deformation scale height* in an *isothermal* atmosphere. The question is whether this scale height still characterises the adjusted state if the atmosphere is not isothermal.

Bannon (1996) extended these results to the nonlinear regime and to an atmosphere of arbitrary thermal structure but, due to the method used, was unable to focus on the deformation scale height in these cases. Neither did he investigate in much detail the transient solution. Sotack and Bannon (1999) generalized Lamb's problem for an isothermal atmosphere to include the effects of heating of finite duration. They invetigated some aspects of the time dependent solution. They found that the duration of the heating, given a certain total heat input, does not affect the final steady state.

This paper complements the above mentioned papers. We will focus on the transient solution. As in Bannon (1995), we will retain the linear assumption. We will however use the Exner function instead of the pressure as a variable, which simplifies the equations considerably, making it possible to derive an equation for the pressure in the final equilibrium state for an atmosphere of arbitrary thermal structure (Section 3). In Sections 4 and 5, we discuss some (numerical) solutions of these equations for an isothermal atmosphere. We find that upward propagating acoustic buoyancy waves attain such great amplitudes in the upper atmosphere that buoyant instability is generated. The parametrization of the breakdown and damping of these waves is discussed in Section 6. In Section 7 the process of hydrostatic adjustment in an atmosphere with a realistic thermal structure is investigated. The paper is concluded in Section 8 with a discussion of the applicability of Lamb's problem to the real atmosphere.

2. The basic equations

Following Lamb (1908) and Bannon (1995), we assume that the atmosphere is homogeneous in the horizontal direction, the motion is inviscid and the earth is flat and not rotating. The equations governing the vertical velocity (w), the potential temperature (θ) and the Exner function (Π) are, assuming the atmosphere is an ideal gas (Van Delden, 1992; Durran, 1999):

$$\frac{\mathrm{d}w}{\mathrm{d}t} = -\theta \frac{\partial \Pi}{\partial z} - g, \tag{2.1a}$$

$$\frac{\mathrm{d}\theta}{\mathrm{d}t} = \frac{J}{\Pi}, \tag{2.1b}$$

$$\frac{\mathrm{d}\Pi}{\mathrm{d}t} = -\frac{R\Pi}{c_\mathrm{v}} \frac{\partial w}{\partial z} + \frac{RJ}{c_\mathrm{v}\theta}, \tag{2.1c}$$

where time, t, and height, z are the independent variables, J is the (diabatic) heating per unit mass, per unit time and c_v is the specific heat at constant volume. The Exner function is related to the pressure, p, by:

$$\Pi \equiv c_\mathrm{p} \left(\frac{p}{p_\mathrm{ref}} \right)^\kappa, \tag{2.2}$$

where p_ref is a reference pressure (here $p_\mathrm{ref} = 10^5$ Pa), c_p is the specific heat at constant volume and κ is the ratio $R/c_\mathrm{p} = (c_\mathrm{p} - c_\mathrm{v})/c_\mathrm{p}$. The potential temperature is defined as,

$$\theta \equiv T \left(\frac{p_\mathrm{ref}}{p} \right)^k = \frac{c_\mathrm{p} T}{\Pi}. \tag{2.3}$$

The set of eqs. (2.1) can be linearised around the steady hydrostatic state of rest (i.e., $\partial \Pi_0/\partial z = -g/\theta_0$ and $w_0 = 0$) by assuming that $\Pi = \Pi_0(z) + \Pi'(z,t)$ and $\theta = \theta_0(z) + \theta'(z,t)$ and $w = w'(z,t)$, where $\Pi' \ll \Pi_0$ and $\theta' \ll \theta_0$, and by neglecting products of perturbation quantities. With $\Gamma \equiv \mathrm{d}\theta_0/\mathrm{d}z$ and dropping primes the system of equations governing the perturbations is:

$$\frac{\partial w}{\partial t} = -\theta_0 \frac{\partial \Pi}{\partial z} + \frac{\theta}{\theta_0} g, \tag{2.4a}$$

$$\frac{\partial \theta}{\partial t} = -\Gamma w + \frac{J}{\Pi_0}, \tag{2.4b}$$

$$\frac{\partial \Pi}{\partial t} = \frac{g}{\theta_0} w - \frac{R\Pi_0}{c_\mathrm{v}} \frac{\partial w}{\partial z} + \frac{RJ}{c_\mathrm{v}\theta_0}. \tag{2.4c}$$

Following Bannon (1995), let us assume that

hydrostatic balance is disturbed at $t=0$ by an intantaneous and vertically confined source of heat. According to eqs. (2.4b) and (2.4c), the amount of heat added per unit mass is $\Pi_0 \mathrm{d}\theta = (c_v\theta_0/R)\,\mathrm{d}\Pi$ (if $w=0$). So, at $t=0$, we must set

$$\Pi(z,t)=\Pi(z,0)=\Pi_i(z)=\left(\frac{R\Pi_0}{c_v\theta_0}\right)\theta_i(z)=\frac{c_0^2}{\theta_0^2}\theta_i(z), \tag{2.5}$$

where

$$c_0\equiv\left(\frac{R\theta_0\Pi_0}{c_v}\right)^{1/2} \tag{2.6}$$

is the phase speed of sound waves in the steady state atmosphere. The subscripts i and f stand for initial and final, respectively. The heat added will perturb both the potential temperature and the pressure. The resulting imbalance will lead to vertical motion. The vertical motion and associated mass divergence will in turn induce further changes in the potential temperature and the pressure, presumably (if $\Gamma>0$) leading to a new state of hydrostatic balance, where

$$w=0,\quad \Pi(z,t)=\Pi(z,\infty)=\Pi_f(z)$$

and

$$\theta(z,t)=\theta(z,\infty)=\theta_f(z),$$

such that

$$\theta_0\frac{\mathrm{d}\Pi_f}{\mathrm{d}z}=\frac{\theta_f}{\theta_0}g. \tag{2.7}$$

3. An equation for the final adjusted state

There is insufficient information to distinguish the correct solution of (2.7) from all (infinite) possible solutions. This "hydrostatic degeneracy" can be removed using an invariant of motion (Bannon, 1995). Assuming that $J=0$, the vertical motion can be eliminated from eq. (2.4c) with eq. (2.4b), yielding:

$$\frac{\partial}{\partial t}\left(\Pi+\frac{g\theta}{\Gamma\theta_0}+\frac{\mathrm{d}\Gamma}{\mathrm{d}z}\frac{c_0^2\theta}{\Gamma^2\theta_0}-\frac{c_0^2}{\Gamma\theta_0}\frac{\partial\theta}{\partial z}\right)=0. \tag{3.1}$$

Therefore,

$$\Pi_f+\frac{g}{\Gamma\theta_0}\left(\theta_f+\frac{\mathrm{d}\Gamma}{\mathrm{d}z}\frac{c_0^2\theta_f}{g\Gamma}-\frac{c_0^2}{g}\frac{\mathrm{d}\theta_f}{\mathrm{d}z}\right)$$
$$=\Pi_i+\frac{g}{\Gamma\theta_0}\left(\theta_i+\frac{\mathrm{d}\Gamma}{\mathrm{d}z}\frac{c_0^2\theta_i}{g\Gamma}-\frac{c_0^2}{g}\frac{\mathrm{d}\theta_i}{\mathrm{d}z}\right). \tag{3.2}$$

In other words, if the initial state is known, the final state can be found from eqs. (2.7) and (3.2), i.e., the degeneracy is removed.

From (2.4a) and (2.4c), we can now easily derive the following equation for Π (assuming $J=0$):

$$\frac{\partial^2\Pi}{\partial t^2}=c_0^2\frac{\partial^2\Pi}{\partial z^2}-g\frac{\partial\Pi}{\partial z}+\frac{g^2}{\theta_0^2}\left(\theta-\frac{c_0^2}{g}\frac{\partial\theta}{\partial z}\right)$$
$$+\frac{c_0^2\Gamma}{\theta_0}\left(\frac{\partial\Pi}{\partial z}+\frac{g\theta}{\theta_0^2}\right). \tag{3.3}$$

In the final steady state, we have

$$c_0^2\frac{\mathrm{d}^2\Pi_f}{\mathrm{d}z^2}-g\frac{\mathrm{d}\Pi_f}{\mathrm{d}z}+\frac{g^2}{\theta_0^2}\left(\theta_f-\frac{c_0^2}{g}\frac{\mathrm{d}\theta_f}{\mathrm{d}z}\right)$$
$$+\frac{c_0^2\Gamma}{\theta_0}\left(\frac{\mathrm{d}\Pi_f}{\mathrm{d}z}+\frac{g\theta_f}{\theta_0^2}\right)=0. \tag{3.4}$$

Using (3.2) and (2.7) to eliminate θ_f and using (2.5) to eliminate Π_i, we find:

$$\frac{\mathrm{d}^2\Pi_f}{\mathrm{d}z^2}+\left(\frac{1}{H_\theta}-\frac{1}{H_N}-\frac{H_\theta}{H_c^2}\right)\frac{\mathrm{d}\Pi_f}{\mathrm{d}z}-\frac{1}{H_c^2}\Pi_f$$
$$=\frac{g}{\theta_0^2}\left(\frac{\mathrm{d}\theta_i}{\mathrm{d}z}-\left(\frac{2}{H_\theta}+\frac{1}{H_N}+\frac{H_\theta}{H_c^2}\right)\theta_i\right), \tag{3.5}$$

where $N^2\equiv g\Gamma/\theta_0$, with N the Brunt–Väisälä frequency, and where:

$$H_\theta\equiv\left(\frac{1}{\theta_0}\frac{\mathrm{d}\theta_0}{\mathrm{d}z}\right)^{-1}=\frac{g}{N^2},\qquad H_N\equiv\left(\frac{1}{N^2}\frac{\mathrm{d}(N^2)}{\mathrm{d}z}\right)^{-1}$$

$$\text{and}\quad H_c\equiv\frac{c_0}{N}, \tag{3.6}$$

are scale heights, determining the adjusted state. Note that the scale height, H_S, introduced in Section 1, is related to the scale heights defined in (3.6) by:

$$H_S=\frac{c_0^2}{\gamma g}=\frac{H_c^2}{\gamma H_\theta}, \tag{3.7}$$

with $\gamma=c_p/c_v$.

Assuming typical tropospheric values for $c_0\simeq 300\ \mathrm{m\,s^{-1}}$, $g\simeq 10\ \mathrm{m\,s^{-2}}$ and $N\simeq 10^{-2}\ \mathrm{s^{-1}}$, we obtain $H_\theta\simeq 100$ km and $H_c\simeq 30$ km, while $H_S\simeq 6$ km. The magnitude of H_N varies by several orders of magnitude and many cases is negative. Note that the scale heights H_θ and H_c increase with decreasing static stability (i.e., decreasing N).

Eq. (3.5) is a 2nd-order inhomogeneous differential equation for $\Pi_f(z)$. The inhomogeneous term on

the r.h.s. of (3.5) is a function of the known initial state. We can simplify eq. (3.5) by substituting:

$$\Pi_f = \Pi_f^* \exp\left(\frac{-1}{2}\int s(z)\,dz\right), \quad \text{with} \quad s(z) = \left(\frac{1}{H_\theta} - \frac{1}{H_N} - \frac{H_\theta}{H_c^2}\right), \tag{3.8}$$

yielding

$$\frac{d^2\Pi_f^*}{dz^2} - A\Pi_f^* = B, \tag{3.9}$$

with

$$A = \frac{1}{2}\frac{ds}{dz} + \frac{1}{4}s^2 + \frac{1}{H_c^2}, \tag{3.10}$$

and

$$B \equiv \exp\left\{\frac{1}{2}\int_0^z s(z')\,dz'\right\} \times \left[\frac{g}{\theta_0^2}\left(\frac{d\theta_i}{dz} - \left(\frac{2}{H_\theta} + \frac{1}{H_N} + \frac{H_\theta}{H_c^2}\right)\theta_i\right)\right]. \tag{3.11}$$

4. The steady solution for an isothermal atmosphere

It can easily be shown that in the special case of an atmosphere with constant temperature T_0, $N^2 = g^2/c_p T_0$. Therefore (see eq. (3.6)),

$$H_\theta = \frac{c_p T_0}{g}, \qquad \frac{1}{H_N} = 0 \qquad \text{and } H_c = \sqrt{\gamma - 1}\,H_\theta. \tag{4.1}$$

Hence, there is only one independent scale height, which, moreover, is independent of z. The parameter, A, in eq. (3.9), thus is constant with height, depending only on the temperature of the atmosphere. From the definition of $s(z)$ in (3.8) together with (4.1) we can deduce that:

$$s(z) = \frac{1}{H_\theta}\left(1 - \frac{c_v}{R}\right). \tag{4.2}$$

From (3.10), we now obtain

$$A = \left(\frac{c_p}{2RH_\theta}\right)^2 = \left(\frac{1}{2H_S}\right)^2. \tag{4.3}$$

The solution of the homogeneous part of (3.9) is:

$$\Pi_f^* = C_1 \exp(\sqrt{A}z) + C_2 \exp(-\sqrt{A}z), \tag{4.4}$$

where C_1 and C_2 are constants, which can be determined from the boundary conditions. The Exner function is then given by (see (3.8)):

$$\Pi_f = C_1 \exp\left(\sqrt{A}z - \frac{1}{2}\int_0^z s(z')\,dz'\right) + C_2 \exp\left(-\sqrt{A}z - \frac{1}{2}\int_0^z s(z')\,dz'\right). \tag{4.5}$$

If the heat source is confined to a finite height, (4.5) is the solution of (3.5) for z corresponding to heights above this heat source, where $B = 0$. The boundary conditions, $\Pi_f = 0$ at $z = 0$ and $\Pi_f = 0$ as z goes to infinity, imply that $C_1 = 0$. With (4.2) and (4.3) we find that the amplitude of the Exner function perturbation in the final state decays with increasing height above the heat source according to:

$$\Pi_f = C_2 \exp\left(-\frac{z}{H_\theta}\right). \tag{4.6}$$

The associated e-folding distance, the scale height for hydrostatic adjustment of the Exner function in an isothermal atmosphere, is

$$a_\Pi = H_\theta. \tag{4.7}$$

For temperatures in the range of approximately 200–300 K, typically measures in the lowest 100 km of the atmosphere, a_Π falls in the range of 20–30 km. In the isothermal atmosphere the scale height for hydrostatic adjustment of the pressure, a_p, is related to a_Π by:

$$a_p = \kappa a_\Pi = H_S. \tag{4.8}$$

When the atmosphere is not isothermal, A in (3.9) is not constant and (3.9) can only be solved numerically.

5. The transition to balance in an isothermal atmosphere

We now investigate the properties of the transient solution for the relatively simple case of an isothermal atmosphere and compare this solution with the numerical solution of (3.9). The linear set of equations (2.4) with $J = 0$ for $t > 0$ is solved numerically, using a forward–backward time stepping scheme on a staggered grid (w and θ are defined on uneven gridpoints and Π is defined on even gridpoints) with boundary conditions, $w = 0$

and $\partial\theta/\partial t = 0$ at $z = 0$ (the first (uneven) gridpoint) and $\partial\Pi/\partial z = 0$ at the top boundary (at $z =$ 400 km). The grid distance is 200 m and initial condition is specified by (2.5), $w_i = 0$ and by:

$$\theta_i = \frac{1}{2}\theta_A\left[1 + \cos\left\{\frac{2\pi[z - \frac{1}{2}(H_1 + H_2)]}{H_2 - H_1}\right\}\right] \quad \text{for } H_1 \leqslant z \leqslant H_2, \qquad (5.1)$$

$$\theta_i = 0 \qquad \text{for } z < H_1 \quad \text{and } z > H_2.$$

This represents a temperature perturbation with an amplitude θ_A confined between $z = H_1$ and $z = H_2$. As an example we choose $\theta_A = 5$ K, $H_1 =$ 20 km and $H_2 = 24$ km, so that there is hydrostatic stability $(\partial\theta_0/\partial z + \partial\theta_i/\partial z > 0)$ everywhere. The timestep is 0.05 s.

Fig. 1 shows the solution at several points in time for an isothermal atmosphere with $T_0 =$ 300 K. In the first few seconds, the heated layer expands and thereby compresses the adjacent air above and below. The pressure rise responsible for compressing the adjacent air does not remain in situ, but propagates upwards and downwards at the speed of sound (347.4 m s^{-1}). The amplitude of the downward propagating perturbation decreases with time while the amplitude of the upward propagating perturbation increases with time. After 58 s, the downward propagating perturbation is reflected at the ground and travels back upwards. We then observe two upward travelling pressure pulses a distance of 44 km apart.

The amplitude of both pulses increases exponentially until either $(\partial\theta_0/\partial z + \partial\theta/\partial z) < 0$ or $(\Pi_0 + \Pi) < 0$ at a particular height. The latter condition would represent a physically impossible state. Fortunately, the former condition (implying buoyant instability) is satisfied first. This happens well into the thermosphere at a height of 138 km at $t = 345.5$ s. Fig. 2 shows the potential temperature perturbation, scaled with the basic state potential temperature, and the gradient of the potential temperature as a function of height at $t = 345.5$ s. We see the two upward travelling negative temperature pulses at heights of 94 km and 138 km, respectively, as well as what is left of the original perturbation, which has adjusted to hydrostatic balance.

Fig. 3 shows the corresponding vertical profile of the Exner function perturbation together with the basic state Exner function, demonstrating that the condition for linearization (i.e., $\Pi \leqslant \Pi_0$) of eq. (2.1c) has been violated at heights above 130 km at this stage of the integration.

Fig. 3 also shows the result of another integration of equations (2.4a, b, c) in which the heating

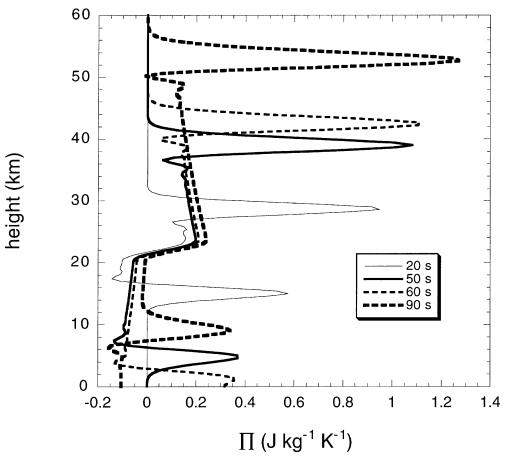

Fig. 1. The solution of the set of eqs. (2.4) with instantaneous initial heating for an isothermal atmosphere at 300 K in terms of the Exner function perturbation as a function of height for different points in time (i.e., $t =$ 20 s, 50 s, 60 s and 90 s, respectively). $\theta_i(z)$ is given by (5.1) with $\theta_A = 5$ K, $H_1 = 20$ km and $H_2 = 24$ km.

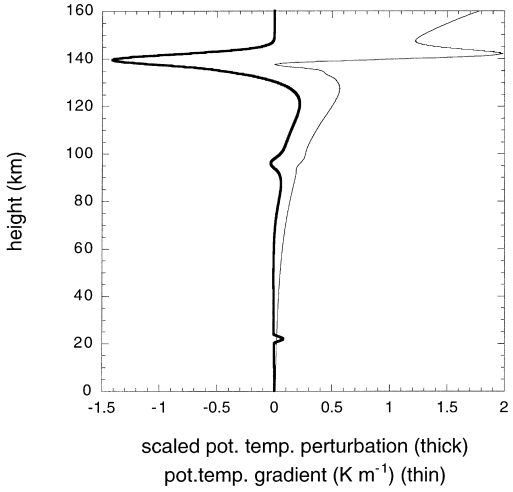

Fig. 2. The potential temperature perturbation, multiplied by 10 and divided by the basic state potential temperature (thick solid line), and the gradient of the potential temperature (thin solid line) in units of K m^{-1} as a function of height at $t = 345.5$ s. See Fig. 1 for further details of this numerical integration.

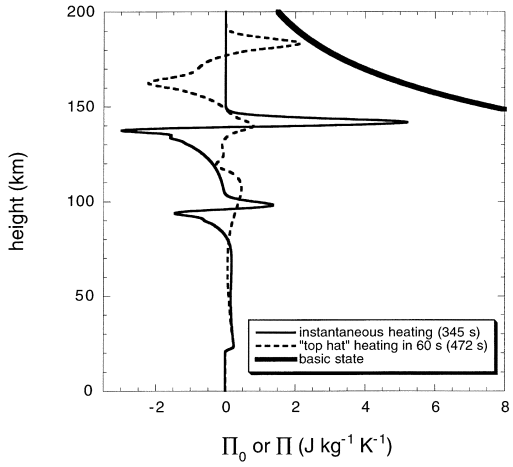

Fig. 3. The Exner function perturbation as a function of height, when the upward travelling acoustic-buoyancy wave first generates buoyant instability. The result of 2 cases is shown, one with instantaneous initial heating (thin solid line; $t = 345.5$ s) and the other with "top hat" heating with $\Delta t = 60$ s (eq. (5.2)) (dashed line; $t = 472$ s). Also shown is the basic state Exner function, Π_0 (thick solid line) ($T_0 = 300$ K).

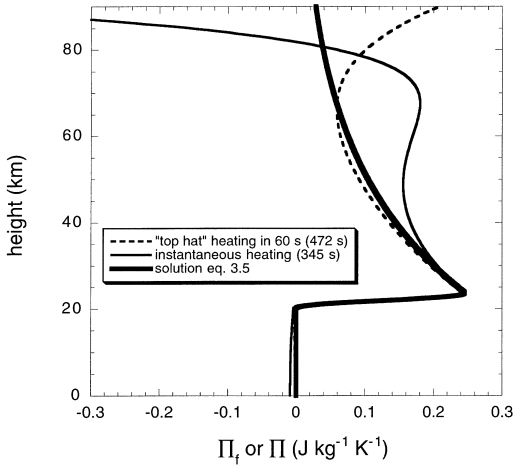

Fig. 4. As Fig. 3, but focussing on the lowest 90 km, together with the corresponding solution Π_f according to eq. (3.5), which should hold for $t \to \infty$ (thick solid line).

is not added instantaneously but is spread over the first 60 s. More specifically:

$$J = \frac{\Pi_0 \theta_i}{\Delta t} \qquad \text{for } t \leqslant \Delta t, \qquad \text{and } J = 0 \text{ for } t > \Delta t, \tag{5.2}$$

with θ_i given by (5.1), $\theta(t=0) = \Pi(t=0) = 0$ and $\Delta t = 60$ s. This represents "top-hat heating" in the terms of Sotack and Bannon (1999). The more gentle application of the heating in this case excites an acoustic-buoyancy wave of smaller amplitude, which therefore travels further upwards before it generates buoyant instability after 472 s.

Fig. 4 demonstrates that the pressure at $z < 40$ km has adjusted quite closely to hydrostatic balance, in accord with the solution given by eq. (3.5). The solutions of eq. (3.5) are obtained by solving eq. (3.9) by the method of succesive over-relaxation on a grid with a grid distance of 200 m. Since $\Pi_f = 0$ for $z \leqslant H_1$ (Bannon, 1996), the boundary condition imposed on the numerical solution is $\Pi_f = 0$ at $z = H_1$ as well as at the upper boundary at a height of 400 km, which is more than $10\times$ greater than the deformation scale height (30 734 m when $T_0 = 300$ K). At $z > 40$ km the atmosphere experiences strong acoustic-buoyancy oscillations.

6. The decay mechanism of acoustic-buoyancy oscillations

What exactly happens when the upward travelling acoustic-buoyancy wave becomes statically unstable is still an unresolved question. It was suggested by Lindzen (1981) that the static instability would generate sufficient turbulence to prevent further wave growth with height. In numerical models designed to simulate vertical propagation of gravity waves a linear Rayleigh damping and a linear Newtonian cooling is frequently added as well as eddy-diffusion, molecular diffusion and fourth or sixth order hyperdiffusion to prevent unstable growth of waves (see, e.g., Zhu et al., 1999). All these dissipation mechanisms are difficult to justify on physical grounds. It is certain that Newtonian cooling is a poor approximation for the radiative drive in the middle atmosphere (Wehrbein and Leovy, 1982).

As a crude first-order estimate of the effect of wave damping on hydrostatic adjustment we now add a term $-\lambda_R w$, representing Rayleigh damping, to the r.h.s. of (2.4a), so that we obtain:

$$\frac{\partial w}{\partial t} = -\theta_0 \frac{\partial \Pi}{\partial z} + \frac{\theta}{\theta_0} g - \lambda_R w, \tag{6.1}$$

instead of (2.4a). This does not alter the invariant of motion (eq. (3.1)), nor does it alter the final steady state (eq. (2.7)). Thus, if the coefficient λ_R

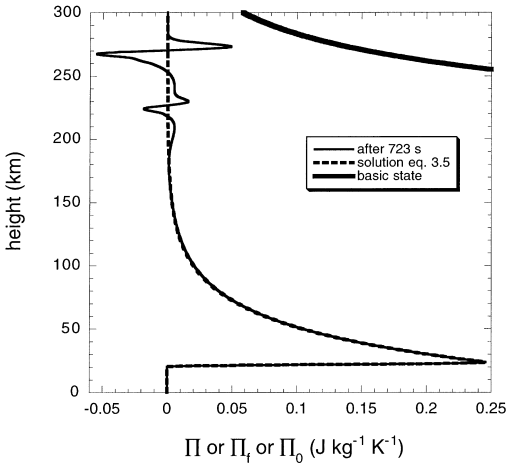

Fig. 5. The Exner function perturbation as a function of height, according to eqs. (2.4b,c) and (6.1) with $\lambda_R = 0.02\ s^{-1}$ at $t = 723$ s (thin solid line) together with the solution Π_f according to eq. (3.5) (dashed line) for an isothermal atmosphere at 300 K. Also shown is the basic state Exner function, Π_0 (thick solid line) ($T_0 = 300$ K).

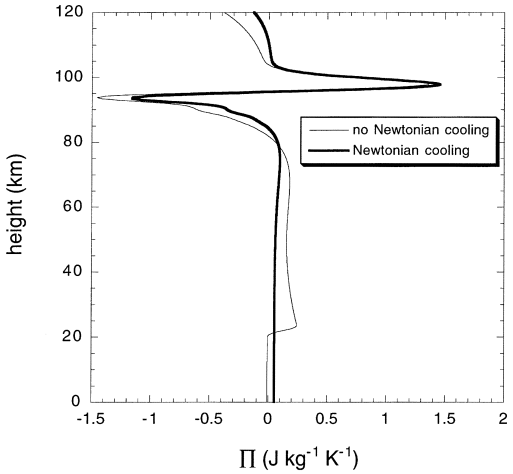

Fig. 6. The Exner function perturbation as a function of height, according to eqs. (2.4a,c) and (6.2) with $\lambda_N = 0.02\ s^{-1}$ (Newtonian cooling, thick line) and with $\lambda_N = 0$ (no Newtonian cooling, thin line) at $t = 345.5$ s ($T_0 = 300$ K).

is large enough, the time dependent solution should converge to the solution of (3.5). In fact, it appears that when $\lambda < 0.01\ s^{-1}$, Rayleigh damping has practically no effect on the solution, in the sense that the waves are damped insufficiently to prevent static instability. For this, a damping period ($1/\lambda_R$) is required which is smaller than the Brunt–Väisälä period of pure buoyancy oscillations (351 s in an isothermal atmosphere at 300 K).

If $\lambda_R = 0.02\ s^{-1}$, the solution becomes statically unstable at $t = 723$ s and $z = 268$ km. However, as can be seen in Fig. 5, below $z = 180$ km the waves are damped completely leaving a solution which is identical to the solution of (3.5). A Rayleigh damping coefficient of $0.02\ s^{-1}$ is, however, three orders of magnitude larger than the usual values found in the literature (Volland, 1988).

The effect of Newtonian cooling on the solution of Lamb's problem is very different to the effect of Rayleigh damping. If we add a term $-\lambda_N\theta$, representing Newtonian cooling, to the r.h.s. of eq. (2.4b), we obtain:

$$\frac{\partial\theta}{\partial t} = -\Gamma w - \lambda_N\theta, \tag{6.2}$$

where λ_N is the Newtonian cooling coefficient. Inspection of eq. (6.2) reveals that a steady state in which $\partial\theta/\partial t = 0$, is now only reached when $\theta = 0$, i.e., when the atmosphere returns to the original basic state (θ_0, Π_0). However, it is the question whether this basic state represents the state of radiative equilibrium.

Let us suppose that the isothermal atmosphere with $T_0 = 300$ K represents the state of radiative equilibrium. We may then repeat the numerical integration with eqs. (2.4a), (2.4c) and (6.2) (i.e., with $\lambda_R = 0$), with $\lambda_N = 0.02\ s^{-1}$. We now find that the waves become hydrostatically unstable after 345.5 s at $z = 138$ km, i.e., at exactly the same time and place as in the case without damping. In Fig. 6, we see that the amplitude of the upward propagating wave is hardly affected by the cooling. However, in the lower atmosphere, the Newtonian cooling has almost completely wiped out the initial temperature perturbation (Fig. 7). Therefore, Newtonian cooling has little or no effect on the acoustic waves in the upper atmosphere and a large effect on the adjustment process in the lower atmosphere.

Several authors (Zhu et al. (1999); see Volland (1988), for older references) have specified Rayleigh damping coefficients and/or Newtonian cooling coefficients which depend on height. In view of the question of the applicability of this kind of parametrization of damping and also in view of the uncertainty of the effect on the waves of the changing composition of the upper atmosphere (above the

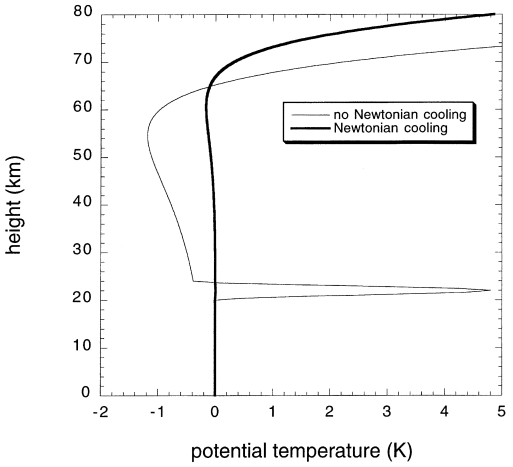

Fig. 7. The potential temperature perturbation as a function of height, according to eqs. (2.4a,c) and (6.2) with $\lambda_N = 0.02\ s^{-1}$ (Newtonian cooling, thick line) and with $\lambda_N = 0$ (no Newtonian cooling, thin line) at $t = 345.5$ s ($T_0 = 300$ K).

turbopause at $z \approx 110$ km), we will not investigate the effect of Rayleigh damping and Newtonian cooling in more detail here. We will introduce Rayleigh damping with the sole practical aim to damp and eliminate the large amplitude acoustic-buoyancy oscillations in the upper atmosphere. More specifically we specify λ_R as follows:

$$\lambda_R = \frac{A}{\pi}\left[\arctan\{B(z - z_T)\} + \frac{\pi}{2}\right], \qquad (6.3)$$

where $A = 0.1\ s^{-1}$, $B = 0.001\ m^{-1}$ and $z_T = 100$ km. Therefore, λ_R is of the order of 10^{-4}–$10^{-3}\ s^{-1}$, in the troposphere, the stratosphere and the mesosphere and abruptly increases to $10^{-1}\ s^{-1}$ above a height of 100 km. Newtonian cooling is not introduced.

7. Adjustment in an atmosphere with a realistic thermal structure

With this parametrization of damping, we now turn to the realistic situation of an atmosphere of variable static stability. We will investigate the effect of heating in the stratosphere as well as the effect of heating near the earth's surface.

Let us consider first the effect of heating in the stratosphere by specifying an initial temperature perturbation as in (5.1) with $\theta_A = 5$ K, $H_1 = 20$ km and $H_2 = 24$ km. This permits a direct comparison of hydrostatic adjustment in an isothermal atmosphere as opposed to hydrostatic adjustment in an atmosphere with a realistic variable thermal structure. We prescribe a piecewise linear temperature profile with $T_0(z = 0) = 300$ K and a temperature gradient, $\partial T_0/\partial z = -0.0065\ km^{-1}$ for $z < 12$ km (the troposphere), $\partial T_0/\partial z = +0.00125\ km^{-1}$ for $12\ km \leqslant z \leqslant 50$ km (the stratosphere), $\partial T_0/\partial z = -0.0025\ km^{-1}$ for $50\ km < z \leqslant 85$ km (the mesosphere) and $\partial T_0/\partial z = +0.0025\ km^{-1}$ for $85\ km < z < 400$ km (the thermosphere).

Fig. 8 shows the solution of eq. (3.5) for the realistic temperature profile and for the isothermal case with $T_0 = 300$ K, together with the solution of the time dependent problem at $t = 7200$ s, when oscillations have practically all vanished (Fig. 9). The solutions are quite similar, the most remarkable difference between the isothermal case and the "realistic" case being the kinks which appear in the vertical profile of the Exner function in the realistic case, reflecting the changes in lapse rate and the associated changes in deformation scale

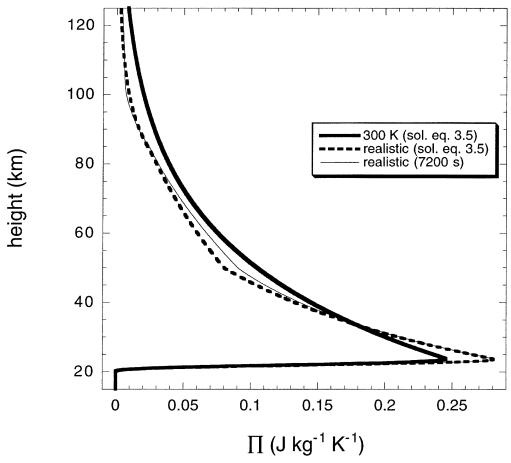

Fig. 8. The Exner function perturbation in the final balanced state as a function of height (i.e., the solution Π_f of eq. (3.5)) resulting from instantaneous initial heating in the stratosphere ($\theta_i(z)$ is given by (5.1) with $\theta_A = 5$ K, $H_1 = 20$ km and $H_2 = 24$ km), for an isothermal atmosphere at 300 K (thick solid line), and for an atmosphere with a realistic stratification (dashed line), together with $\Pi(z, t)$ for an atmosphere with a realistic stratification (including Rayleigh damping according to eqs. (6.1) and (6.3)) for $t = 7200$ s (thin solid line).

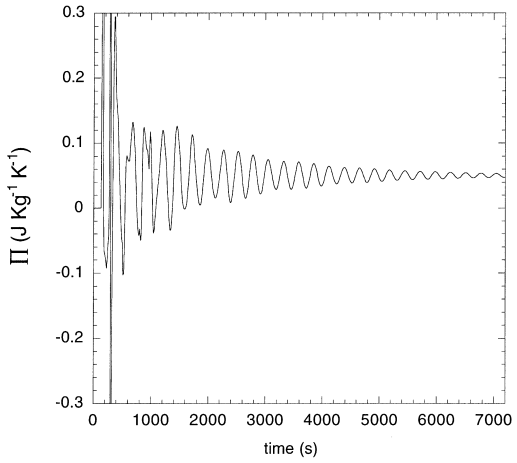

Fig. 9. The Exner function perturbation $\Pi(z, t)$ at $z =$ 70 km for the integration with instantaneous initial heating in the stratosphere. See Fig. 8 for further details.

height (see eq. (3.6) and the discussion below). We will return to this point at the end of this section.

The amplitude of the oscillations in the time dependent solution (Fig. 9) remains large compared to the amplitude of the steady state solution for at least the first hour of integration. The period of these oscillations for $t > 1$ h is approximately constant (about 270 s). This can be explained by observing the dispersion relation which results when we substitute solutions of the form:

$$\begin{bmatrix} \Pi \\ w \\ \theta \end{bmatrix} = \begin{bmatrix} P(z) \\ W(z) \\ \Theta(z) \end{bmatrix} \exp\{-i\omega t\} \tag{7.1}$$

into eqs. (2.4a–c). In (7.1) P, W, Θ, are z-dependent amplitudes and ω is the frequency. Assuming, for simplicity, that $\Pi_0 \approx \Pi_m =$ constant and $\theta_0 \approx \theta_m =$ constant, and that $\Gamma =$ constant and $J = 0$ (adiabatic conditions), the dispersion relation is:

$$\omega^2 = N^2 + c_m^2 k^2 + \frac{1}{4}\frac{g^2}{c_m^2}, \tag{7.2}$$

where

$$c_m = \left(\frac{R\theta_m \Pi_m}{c_v}\right)^{1/2}, \tag{7.3}$$

and

$$W(z) = C \exp\left(ikz + \frac{1}{2}\frac{g}{c_m^2} z\right), \tag{7.4}$$

with k the vertical wavenumber and C an amplitude. Eq. (7.2) demonstrates that the frequency of oscillations is greater than the Brunt–Väisälä frequency and that the group velocity of acoustic-buoyancy waves in this one-dimensional model approaches zero when the wavenumber approaches zero. The waves with small wavelengths will propagate upwards into the thermosphere and will be damped, while the waves with large wavelengths will hardly propagate vertically and the associated oscillations will be noticed in the lower atmosphere for a relatively long time. The frequency of these oscillations is

$$\omega \simeq \left(N^2 + \frac{1}{4}\frac{g^2}{c_m^2}\right)^{1/2}. \tag{7.5}$$

At $z = 70$ km, where $N \approx 0.018\ \mathrm{s}^{-1}$ and $c_m \approx 300\ \mathrm{m\ s}^{-1}$, this would result in a frequency, $\omega \approx 2.46 \times 10^{-2}\ \mathrm{s}^{-1}$, or equivalently, a period of oscillation of about 255 s, which agrees approximately with the frequency observed in Fig. 9.

As an illustration of the time needed for hydrostatic adjustment, Fig. 10 shows the Exner function perturbation as function of height at $t = 450$ s, at $t = 1$ h and at $t = 4$ h, respectively, in a numerical integration in which an instantaneous heat source

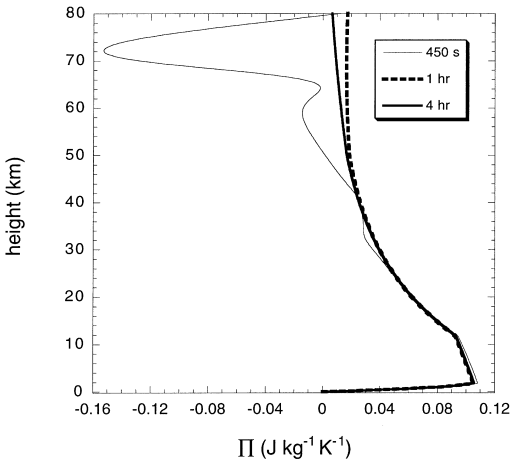

Fig. 10. The Exner function perturbation $\Pi(z, t)$ (including Rayleigh damping according to eqs. (6.1) and (6.3)) at $t = 450$ s, $t = 1$ h and $t = 4$ h, respectively, for instantaneous initial heating in the lowest 2 km of the atmosphere ($\theta_i(z)$ is given by (7.6) with $\theta_s = 1$ K and $H =$ 2 km) for an atmosphere with a realistic stratification.

was prescribed in the boundary layer such that

$$\theta_i = \theta_s\left(1 - \frac{z}{H}\right) \qquad \text{for } z \leqslant H, \qquad \theta_i = 0 \qquad \text{for } z > H, \tag{7.6}$$

with $H = 2$ km and $\theta_s = 1$ K.

We see in Fig. 10 that the atmosphere below a height of about 40 km is close to the steady balanced state after 450 s. The perturbation in the Exner function is equal to zero at the ground and increases to a maximum of slightly over 0.1 J kg^{-1} K^{-1} at $z = 2$ km. Above this height there is a relatively slow decay of the Exner function perturbation with height within the troposphere, where the static stability is relatively weak and the deformation scale height is relatively large, and a much quicker decay with height within the almost isothermal stratosphere where the deformation scale height is smaller.

8. Conclusion

We have investigated the linear dynamics of hydrostatic adjustment in a horizontally homogeneous atmosphere, using the analytical techniques introduced by Gill (1982) and Bannon (1995) and using numerical methods. In particular, we have investigated the reaction of the atmosphere to an instantaneous source of heat. We have derived an equation for the Exner function (or pressure) in the final equilibrium for an atmosphere of arbitrary thermal structure. The analytical solution of this elliptic equation is only possible for an isothermal atmosphere. We have compared numerical solutions of this equation with time-dependent solutions obtained by integrating the original equations in time.

High-frequency acoustic waves play a key rôle in hydrostatic adjustment, similar to the role played by high frequency gravity waves in geostrophic adjustment (Gill, 1982). However, in the case of hydrostatic adjustment, the amplitude of these waves increases exponentially as they propagate upwards creating static instability and thus preventing the atmosphere (in particular, the upper atmosphere) from reaching a steady state.

When Rayleigh damping is added to the momentum equation, as a crude parametrization of the unstable breakdown of these waves, the oscillations ultimately vanish and the lower part of the atmosphere (the troposphere and the stratosphere) adjusts to near hydrostatic balance in several minutes, depending on the damping coefficient and the phase speed of acoustic waves, which play the role of "transporting" the imbalance away from the source region.

The principle limitations of the model problem discussed in this paper are due to the neglect of nonlinear effects and the neglect of horizontal inhomogeneities. Nonlinear effects are not important in the troposphere and the stratosphere, due to the small amplitude of the acoustic buoyancy waves, but obviously cannot be neglected when these waves attain large amplitudes in the mesosphere and thermosphere.

To appreciate the limitations introduced by the neglect of horizontal inhomogeneities, it is worthwhile to imagine what would happen if the heating were not horizontally homogeneous, but were limited to a circular area with a radius, r. The heating would then not only excite a vertically propagating horizontal wave-front above the heated area, but also a horizontally and vertically propagating circular wave-front at the outer edge of the heated area. Due to its horizontal propagation, the latter wave-front would affect the one-dimensional (vertical) hydrostatic adjustment process (investigated in this paper) in the centre of the heated area after a time in the order of r/c_0. If $r \approx 300$ km, this would be after about 15 min. Since the purely vertical adjustment proces within the troposphere and the stratosphere takes in the order of 10 min (Fig. 10), we may conclude that the problem first discussed by Lamb (1908) and much later taken up by Bannon (1995, 1996), Sotack and Bannon (1999) and finally elaborated upon further in this paper is relevant for homogeneous heating over regions with a horizontal scale of at least several hundred km. The obvious next step is to investigate the effect of horizontal inhomogeneities in heating. Some aspects of this problem, with application to the sea breeze, have already been investigated by Tijm and Van Delden (1999).

9. Acknowledgements

I would like to thank Huib de Swart for advice on mathematics and numerics and Sander Tijm for advice on numerics. I am also indebted to Peter Bannon for very helpful criticism.

REFERENCES

Bannon, P. R. 1995. Hydrostatic adjustment: Lamb's problem. *J. Atmos. Sci.* **52**, 1743–1752.

Bannon, P. R. 1996. Nonlinear hydrostatic adjustment. *J. Atmos. Sci.* **53**, 3606–3617.

Delden, A. van, 1992. The dynamics of meso-scale atmospheric circulations. *Physics Reports* **211**, 251–376.

Durran, D. R. 1999. *Numerical methods for wave equations in geophysical fluid dynamics*. Springer-Verlag, New York, 465 pp.

Gill, A. E. 1982. *Atmosphere–ocean dynamics*. Academic Press, New York, 662 pp.

Lamb, H. 1908. On the theory of waves propagated vertically in the atmosphere. *Proc. London Math. Soc.* **7**, 122–141.

Lamb, H. 1932. *Hydrodynamics*, 6th edition, 1945. Dover, New York, 738 pp.

Lindzen, R. S. 1981. Turbulence and stress owing to gravity wave and tidal breakdown. *J. Geophys. Res.* **86C**, 9707–9714.

Sotack, T. and Bannon, P. R. 1999. Lamb's hydrostatic adjustment for heating of finite duration. *J. Atmos. Sci.* **56**, 71–81.

Tijm, A. B.C. and van Delden, A. 1999. The role of sound waves in sea breeze initiation. *Q. J. R. Meteorol. Soc.* **125**, 1997–2018.

Wehrbein, W. M. and Leovy, C. B. 1982. An accurate radiative heating and cooling algorithm for use in a dynamical model of the middle atmosphere. *J. Atmos. Sci.* **39**, 1532–1544.

Volland, H. 1988. *Atmospheric tidal and planetary waves*. Kluwer Academic Publishers, Dordrecht, 348 pp.

Zhu, X., Yee, J.-H., Strobel, D. F., Wang, X. and Greenwald, R. A. 1999. On numerical modelling of middle atmosphere tides. *Q. J. R. Meteor. Soc.* **125**, 1825–1857.